polariton because of the coating thin-film metal is excited at the aperture rim by the evanescent photons and propagates nearly parallel to the sample surface, resulting in enlargement of the spot size. Since the electric flux density is conserved, the electric field amplitude is greater than the external medium where the permittivity is smaller. Considering the boundary condition, the incident wave should have a component vertical to the subwavelength circular aperture in an infinite aluminum thin plate at the output edge of the aperture in order to excite the localized-mode surface plasmon.39) Fig. 2(c) and (d) shows the same as Fig. 2(a) and (b) except that the illumination is s-polarized. In the central part of this model, the electric intensity is stronger than those in other region of the model. Besides, it is found that the decrease in the images contrast relative to the image shown in Fig. 2(a) and (b). In this case, the s-polarization is responsible for the surface digging. The estimated digging of the surface after illumination by a metallized aperture with s-polarization is similar to the experimental surface deformation in good agreement with current experimental data. The main differences between the two principal polarizations are hence the degree of confinement which is favorable for s-polarization and the available electric field distribution which is favorable for p-polarization. It is important to remark here that the intensity of p-polarized field plays a leading role for edge enhancement. If we come back to the field maps of Fig. 2 (a)-(d), we see the light is generated mostly by the aperture rim in p-polarization, coming from the excitation of the metal coating and the apparition of a local dipole along the rim of aperture. On the contrary, for s-polarization, there is a lot of light at the central part of aperture, is responsible for the surface digging.

4.3.2 The 3-D NSOM image of dielectric tip

As a matter of fact, the perspective of improving the optical data storage is a big challenge at the beginning of a communication century. Different methods were then investigated to reach this aim, with various efficiencies. The illumination probe can be a dielectric probe,[4] a coated one,[40] or even a STM tip.[41] The possible photosensitive samples are numerous, from the magneto-optical sample[42] to the liquid-crystal layer.[43] Various parameters are involved and a lot of progress has still to be realized to control them. We will compare the non-coated (purely dielectric tip) with metal coated tip here. The two tips can also be used as an optical pickup for a data storage system to realize very high density data recording. Performance of NSOM or data storage system depends on the optical properties of the near-field tip. Both high throughput (light efficiency) and resolution (smaller spot size) are desired. In transmission illumination mode-NSOM allows the radiative optical wave to be converted into the confined wave concentrated near the probe apex.

Fig. 3 (a) and (b) shows a sectional plane diagram of 3-D NSOM model of dielectric tip and metal- coated tip, respectively, which probe-sample interactions are taken into account in

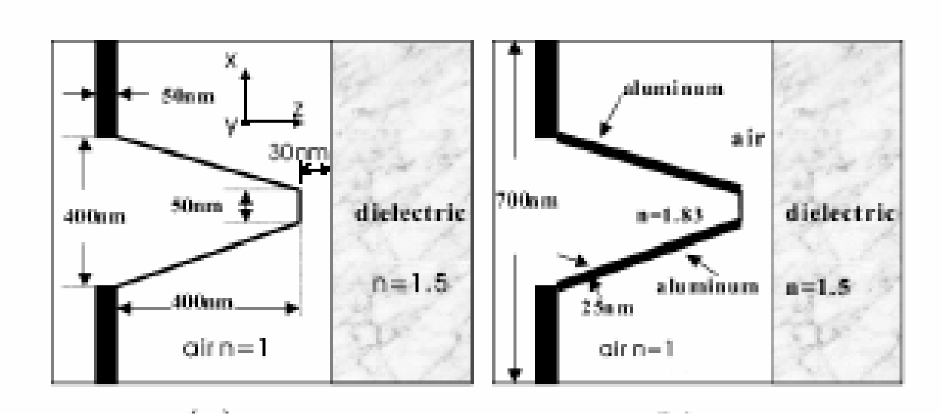

Fig. 4.3 The sectional plane diagram of 3-D NSOM model, (a) for a dielectric tip and (b) for a tip coated with metal, respectively, which probe-sample interactions are taken into account.

order to realize the field distribution formed by the probe tip. In Fig. 3(a), the dielectric probe tip exhibits the profile of a cone and has height of 400nm, an aperture opening of 50 nm (10 cells) at the apex, 400 nm (80 cells) at the bottom of the probe. We choose to model an acute tip, with half-angle slope of the tip is 23.60. The material of the probe is purely dielectric with the refractive index of 1.83 except for a thin (50nm) metal film screen at its bottom face that is assumed to center the incident beam to the axis of the tip. In front of the probe, at a distance of 30 nm (6 cells) a semi-infinite silicon medium was taken as the sample with the refractive index of n=1.5. The dimensions of each cell is $\Delta x=\Delta y=\Delta z=\Delta=5$nm, and the entire region model is 140(x) × 140(y) ×140(z) cells. In the experiments, the three-dimensional probes support both polarizations simultaneously. The output field distribution of tip will be small as their tip size decreases. Thus it is expected that the optical power density of field distribution has maximum density at a certain area of the tip due to the focusing effect by reflection on the internal surface of conic shape of the tip. Figs. 4(a)-(d) show the calculated results in x-z sectional plane (at $y=70\Delta$) and y-z sectional plane (at $x=70\Delta$) for p-polarization and s-polarization illumination, respectively. Results show good agreement with the experimental report by Hans et.[44] As expected, the field intensity decreases rapidly near the probe tip due to the light wave converts to radiation mode or is returned back by the reflection. That is to say, the incident wave, coming from the base plane to the tip, propagates inside the tip as far

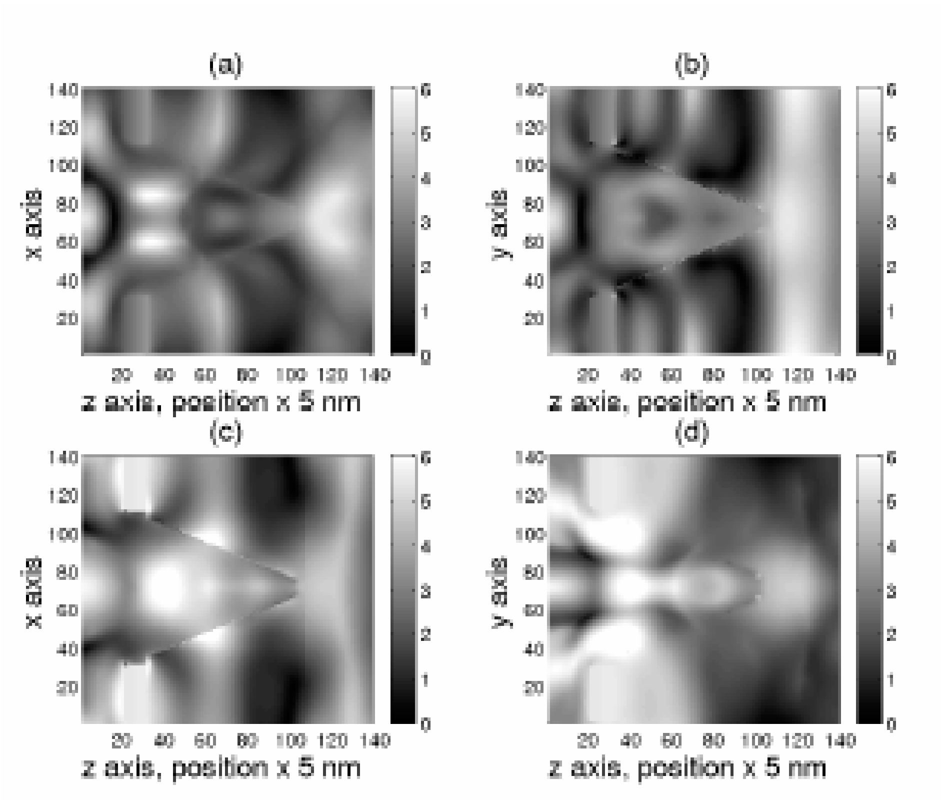

Fig. 4.4 Distribution of the 3-D electric field intensity modulus around the tip-sample coupling zone (dielectric tip): (a)in x-z plane (at y=70 △), p-polarization, (b)in y-z plane (at x=70 △), p-polarization, (c)in x-z plane (at y=70 △), s-polarization, and (d)in y-z plane (at x=70 △), s-polarization, respectively. The electric field resulting from an incident wave coming from the left side.

as the diameter of the conic shape of tip is wide enough. Once the propagation becomes too difficult, more and more light escapes from the lateral surfaces limiting the tip. These far-field components will contribute to illuminate on a large spatial zone. The light generated by the apex of the tip is essentially evanescent, since most propagating components escaped laterally before reaching the coupling zone. The near-field effect is confined to the surface area located in front the tip extremity. In this region the illumination process is mainly supported by evanescent fields. The distribution of the field intensity along the surface is similar to the field distribution obtained when an incident field is diffracted by a subwavelength aperture. Based on our simulation in this case, we find the electric field leaking from the conic side is much stronger than the emerging one from the tip apex for non-coated (purely dielectric) probes. The reflected light from the conic surface inside the probe couples with the incident light to become the incomplete standing wave and escapes from the lateral surfaces as long as the diameter of conic shape approximately less than 180 nm. These will contribute far-field component.

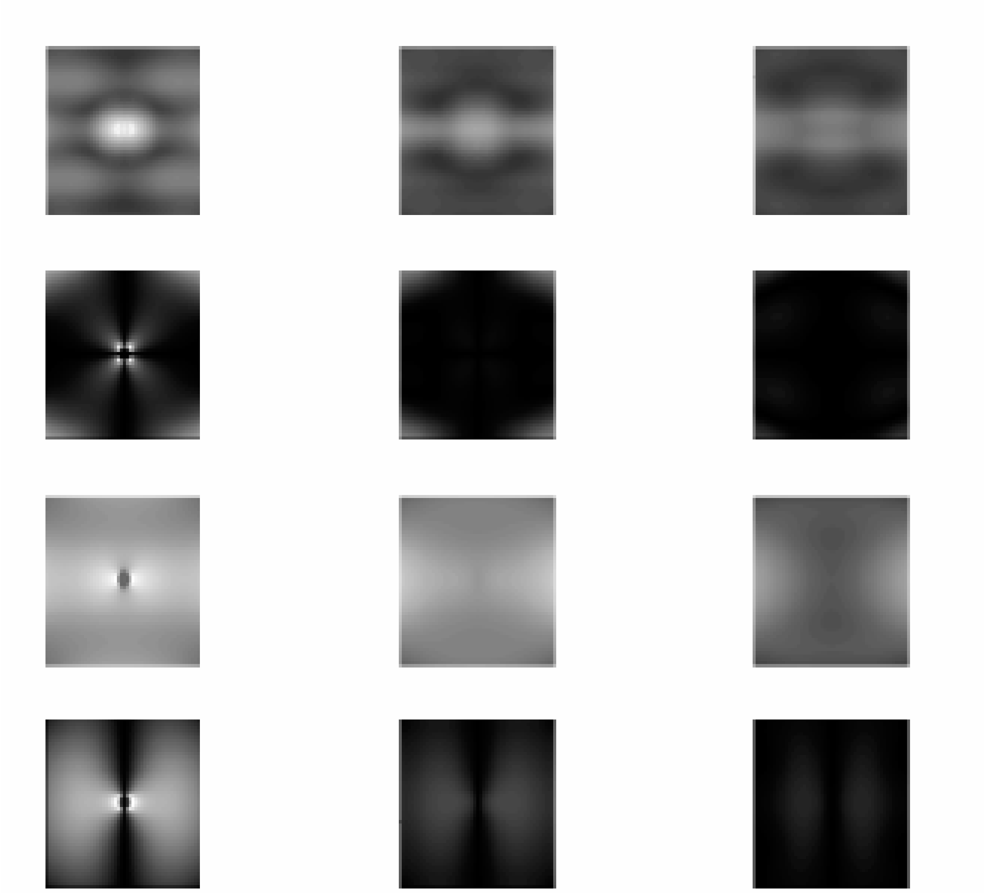

Fig. 4.5 Distributions of total electric-field and field components without sample interactions for p-polarization illumination in the plane away from probe apex of z= 5nm,15nm,30nm (from left to right), respectively. From top to bottom : $|E_t|$, $4\times|Ex|$, $|E_y|$, $|Ez|$, respectively. The size of each image plane displayed is 700×700 *nm*2 in front of the probe.

By the way, the depolarization phenomenon of electric field components is important in the near-field zone. The dielectric tip declines the polarized incident wave, namely the emerging light from the tip lose the characteristics of polarization, after exiting from the tip apex, produces two perpendicularity polarized electric-field components, that is the incident field is entirely polarized along the y-axis, the scattered field has also been divided into the components of the electric fields along the x-axis, z-axis, respectively. These two components produce depolarization at this interface between the probe tip and the air. Fig. 5 shows the distributions of total electric-field without sample interactions in x-y sectional plane for p- polarization illumination and the field components in the plane away from probe apex of z=5nm,15nm,30nm (from left to right). From top to